



# RESEARCH MEMORANDUM

EXPERIMENTAL AND THEORETICAL AERODYNAMIC CHARACTERISTICS  
OF TWO LOW-ASPECT-RATIO DELTA WINGS AT ANGLES OF  
ATTACK TO  $50^\circ$  AT A MACH NUMBER OF 4.07

By Fred M. Smith

Langley Aeronautical Laboratory  
Langley Field, Va.

**NATIONAL ADVISORY COMMITTEE  
FOR AERONAUTICS**

WASHINGTON

July 10, 1957  
Declassified July 11, 1961

## NATIONAL ADVISORY COMMITTEE FOR AERONAUTICS

---

RESEARCH MEMORANDUM

---

## EXPERIMENTAL AND THEORETICAL AERODYNAMIC CHARACTERISTICS

OF TWO LOW-ASPECT-RATIO DELTA WINGS AT ANGLES OF

ATTACK TO  $50^\circ$  AT A MACH NUMBER OF 4.07

By Fred M. Smith

## SUMMARY

An investigation has been conducted in the Langley 9- by 9-inch Mach number 4 blowdown jet to determine the aerodynamic characteristics of two double-wedge-section delta wings of aspect ratio 1.3 and 2.3 to angles of attack of  $50^\circ$  at a Mach number of 4.07 and Reynolds numbers of 6.0 and  $5.3 \times 10^6$ , respectively. The results of the investigation are compared with the predictions of linear theory, two-dimensional shock-expansion theory, Newtonian-impact theory, and a method which utilizes the shock-wave and expansion-wave equations expanded by the two-dimensional hypersonic-flow similarity parameter. Linear theory, although fortuitously, generally gives the best predictions for all components.

The results of this investigation extend a trend established in lower Mach number tests that the maximum lift coefficient for low-aspect-ratio delta wings decreases with increasing Mach number. The results also extend to a Mach number of 4.07 the trend indicated by lower Mach number tests that the angle of attack for maximum lift coefficient increases with increasing Mach number.

## INTRODUCTION

Numerous experiments have been made to determine the supersonic aerodynamic characteristics of low-aspect-ratio delta wings at low and moderate angles of attack (for example, refs. 1 to 5). Relatively few tests have been made, however, at high angles of attack (above an angle of attack of  $30^\circ$ ) and these data are limited to a maximum Mach number of 3.36 (refs. 6 to 8 and unpublished data obtained at the Ames Aeronautical Laboratory). This shortage of high-angle supersonic data leaves the designer with no empirical results upon which to base his predictions of the maximum lift and other wing characteristics at high

angles. It also precludes a comparison of theoretical methods with experimental results to determine which theoretical methods best predict the high-angle-of-attack and high Mach number wing characteristics.

The present investigation, instigated by the lack of experimental data, was conducted on two low-aspect-ratio (1.33 and 2.31) double-wedge-section delta wings in the Langley 9- by 9-inch Mach number 4 blowdown jet. In this investigation, normal force, chord force, pitching moment, and wing-root bending moment were obtained for angles of attack from  $-4^{\circ}$  to  $50^{\circ}$  at a Mach number of 4.07 and Reynolds numbers of  $5.3 \times 10^6$  and  $6.0 \times 10^6$  based on the wing mean aerodynamic chords.

The experimental results were compared with the predictions of linear theory, two-dimensional shock-expansion theory, Newtonian-impact theory, and a method by Dorrance (ref. 9) wherein the shock-wave and expansion-wave equations are expanded by the two-dimensional hypersonic flow similarity parameter.

#### SYMBOLS

A	aspect ratio
B	wing-root bending moment, positive with positive lift
b	wing span, twice semispan
c	wing-root chord
$\bar{c}$	wing mean aerodynamic chord, $2/3 c$
$C_b$	wing-root bending-moment coefficient, $2B/qSb$
$C_D$	drag coefficient, $D/qS$
$C_{D0}$	drag coefficient at zero angle of attack
$C_L$	lift coefficient, $L/qS$
$C_{L_{max}}$	maximum lift coefficient
$C_{L\alpha}$	lift-curve slope, $\alpha = 0^{\circ}$
$C_m$	pitching-moment coefficient, $M/qSc$

$C_N$	normal-force coefficient, $N/qS$
$D$	drag force
$K$	hypersonic similarity parameter, $M_\infty \delta$
$L$	lift force
$m$	Mach angle
$M$	pitching moment about $0.5\bar{c}$
$M_\infty$	free-stream Mach number
$N$	normal force
$q$	free-stream dynamic pressure
$R$	Reynolds number based on wing $\bar{c}$
$S$	area of semispan wing
$t$	wing thickness
$\alpha$	angle of attack
$\alpha_{C_{L_{\max}}}$	angle of attack for maximum lift
$\delta$	thickness ratio, $t/c$
$\epsilon$	wing semiapex angle

## APPARATUS AND TESTS

The tests were conducted in the Langley 9- by 9-inch Mach number 4 blowdown jet. A description of the jet along with a test-section flow calibration is presented in reference 10. The settling-chamber pressure, which was held constant by a pressure regulating valve at approximately 13 atmospheres, and the corresponding air temperature, which dropped from 75° F to approximately 30° F, were both continuously recorded during each test. This pressure and temperature range resulted in average test Reynolds numbers, based on wing mean aerodynamic chords, of  $5.3 \times 10^6$  and  $6.0 \times 10^6$ .

An external sidewall-mounted strain-gage balance was used to measure the normal force, chord force, pitching moment, and wing-root bending moment of the two wings. The models were mounted as shown schematically in figure 1 to eliminate the effects of the tunnel-wall boundary layer and to minimize the gap around the root of the model. Surveys have indicated that the sharp-leading-edge boundary-layer scoop-off plate has almost negligible effects on the air stream in the tunnel. Such effects have been computed to fall easily within the accuracy of the experimental data. The tests were made for an angle-of-attack range of  $-4^{\circ}$  to  $50^{\circ}$  at a Mach number of 4.07.

The tests were made at humidities below  $5 \times 10^{-6}$  pounds of water vapor per pound of dry air; these humidities should be low enough to eliminate water-condensation effects. The test-section static temperature and pressure did not reach values for which liquefaction of the air would occur.

#### MODELS

The models consisted of two steel semispan delta wings having, respectively, semiapex angles of  $18.4^{\circ}$  and  $30^{\circ}$ , aspect ratios of 1.33 and 2.31, and double-wedge sections 8 percent and 5 percent thick. The wings are shown in schematic form as figure 2.

#### PRECISION OF DATA

The maximum inaccuracies of the experimental angles, forces, and moments due to balance and recording equipment limitations, and the average repeatability of the system have been estimated and are presented in the following table:

Value	Accuracy
$\alpha$ . . . . .	$\pm 0.1$
$C_L$ . . . . .	$\pm 0.010$
$C_D$ . . . . .	$\pm 0.010$
$C_{D0}$ . . . . .	$\pm 0.001$
$C_m$ . . . . .	$\pm 0.005$
$C_b$ . . . . .	$\pm 0.016$
$M_{\infty}$ . . . . .	$\pm 0.02$

The data are generally felt to be more accurate than the given values.

## THEORETICAL METHODS

Predictions of lift, drag, and centers of pressure were made for the two wings by linear theory (as in ref. 1), two-dimensional shock-expansion theory (ref. 11), Newtonian-impact theory (as applied in ref. 12), and Dorrance's method (ref. 9). Each of the drag predictions contains the same friction drag coefficient estimated from references 13 and 14.

## Linear Theory

It is realized that, for the Mach number and angles of attack of the present tests, linear theory is not strictly applicable because linear theory applies to slender wings at small angles. It has been shown in other high Mach number, high-angle investigations, however, that certain compensating factors are present so that, when the linear-theory slopes are extended to high angles, good resultant-force agreement is obtained from poor distribution agreement (refs. 6, 7, 8, and 15). It was to see whether the same compensating factors were present at higher Mach numbers and angles of attack that comparisons of linear-theory predictions are made with the present experimental results.

## Shock-Expansion Theory

Predictions of the two-dimensional shock-expansion theory have been shown to give good agreement with the lift-curve slope and wave drag for sharp-leading-edge delta wings having attached leading-edge shock waves. (See refs. 16 and 17.) The wings of the present investigation do not fall within the restriction of the theory that the leading-edge shock waves must be attached because the lower aspect-ratio wing, designated as wing 1, has such a large effective thickness that the leading-edge shock wave is detached even at  $\alpha = 0^\circ$ , and the leading-edge shock for wing 2 becomes detached at  $\alpha = 10^\circ$ . The shock-expansion predictions are given, nevertheless, for both wings to the angle for two-dimensional shock detachment to determine whether, as with the linear-theory predictions, compensating factors exist that give a reasonable approximation of the resultant forces or slopes of the force curves outside the region of applicability of the theory.

## Newtonian-Impact Theory

Bertram and McCauley (ref. 12) found that Newtonian theory ( $2 \sin^2 \alpha$ ) gave fairly good lift predictions for low-aspect-ratio delta wings ( $\epsilon < 22^\circ$ ) with rather large thicknesses having detached leading-edge shock waves between Mach numbers of 1.6 and 6.9. For higher aspect-ratio

wings with either attached or detached leading-edge shock waves, Bertram and McCauley found that two-dimensional shock-expansion theory gave better predictions. Since one wing of the present tests fell in each category, it was desirable to obtain theoretical predictions by both methods for the two wings.

#### Dorrance's Method

In reference 9 Dorrance derives aerodynamic coefficient expressions for airfoil sections in two-dimensional hypersonic flow which gave good agreement with experimental results for some three-dimensional wings having sections similar to those of the present test wings. The method employs the shock-wave and expansion-wave equations which are ordinarily used to determine the pressure ratios across the waves and expands them in terms of the two-dimensional hypersonic-flow similarity parameter  $K$  ( $K = M_\infty \delta$ ). This method is restricted to  $M_\infty \geq 3.19$  and maximum angles of attack of approximately  $1/M_\infty$ .

The method strictly applies only for the higher aspect-ratio wing 2 to the angle for shock detachment but, for comparison purposes, it is presented for both wings to the angle for two-dimensional-shock detachment.

#### Van Driest's Skin-Friction Method

A skin-friction drag from Van Driest's theoretical methods for obtaining laminar and turbulent skin-friction coefficients (refs. 13 and 14) is combined with each of the pressure-drag predictions presented in this discussion to obtain total-drag predictions. In applying Van Driest's methods, the turbulent boundary layer after transition from laminar flow was assumed to be the same as if the boundary layer had been turbulent the entire distance up to the transition points. These transition points for the two wings were determined experimentally from fluorescent-lacquer boundary-layer-visualization tests. (See fig. 3.) The skin friction for the laminar boundary layer ahead of this transition point and the turbulent boundary layer behind it were then combined according to equation (6) of reference 2. This total skin-friction drag, when applied, was assumed to be constant throughout the angle-of-attack range.

### RESULTS AND DISCUSSION

The aerodynamic data for the two test wings are presented as functions of angle of attack in figures 4 to 9. The data were obtained at

Reynolds numbers of  $6.0 \times 10^6$  and  $5.3 \times 10^6$  for the aspect-ratio-1.33 wing (designated as wing 1) and the aspect-ratio-2.31 wing (designated as wing 2), respectively.

#### Normal-Force and Lift Results

The normal-force and lift results for the two wings, shown in figures 4 and 5, were almost as would be expected from lower Mach number tests. The one unanticipated variation from previous tests was that  $C_{L_{max}}$  was not attained even at  $\alpha = 50^\circ$ . In order to obtain an indication of  $C_{L_{max}}$ , the normal-force curves were first extrapolated about 10 percent as shown in figure 4. The lift components of these normal-force curves ( $C_N \cos \alpha$ ) were then plotted as the solid lines in figure 5; by the proximity of these lines to the actual lift points, the normal-force component of the lift is shown to be significant and the chord-force component insignificant. This result, together with the approximate linearity of the normal-force curves at the high angles of attack, was the justification for using the extrapolated  $C_N \cos \alpha$  for an indication of  $C_{L_{max}}$  for both wings.

References 6 and 18 present trends showing that  $C_{L_{max}}$  for low-aspect-ratio delta wings decreases with increasing Mach number. The present results conform with this trend and extend it to  $M = 4.07$  (see fig. 10(a)).

Another trend indicated by the present test data in conjunction with lower Mach number data is that the angle of attack at which  $C_{L_{max}}$  is obtained ( $\alpha_{C_{L_{max}}}$ ) increases with increasing Mach number from about  $41^\circ$  at  $M = 1.5$  to  $54^\circ$  at  $M = 4.0$ . (See fig. 10(b).)

Of the theoretical methods used for comparison, it is seen in figure 5 that linear theory gives the best overall lift prediction to the point of maximum lift for both wings. This agreement indicates that linear theory may be useful in predicting lift up to  $M = 4.07$ . It should be remembered, however, as pointed out in the "Theoretical Methods" section that comparisons of linear theory with experimental data up to  $M = 3.36$  (refs. 6, 7, 8, and 15) showed that, although lift predictions were good, the pressure distributions were usually very poor.

The Newtonian-impact theory, although low in its lift predictions, does predict the trends of the lift curves including  $\alpha_{C_{L_{max}}}$ . With the exception of Newtonian-impact theory, all the theoretical methods predicted the experimental  $C_{L_{\alpha}}$  within 26 percent for wing 1 and within 4 percent for wing 2. (See table I.) The poorer predictions for wing 1 no doubt occurred because the leading-edge shock was detached even at  $\alpha = 0^\circ$ .

### Drag Results

The drag results are presented in figure 6 as a function of angle of attack. If the Newtonian-impact theory once more be excepted, because of its very low prediction, the remaining theoretical methods are shown in table I to predict the experimental minimum drag within 26 percent for wing 1 and within 7 percent for wing 2. It may also be seen from table I that the linear theory  $C_{D0}$  for wing 1 shows the greatest disagreement of the remaining methods. This disagreement is in accordance with reference 16 which shows that, for double-wedge delta wings with  $\frac{\tan \epsilon}{\tan m} < 1.5$ , the experimental  $C_{D0}$  is much lower than the unrealistic peaks of the linear-theory curve. For both wings the drag is best predicted by linear theory throughout the angle-of-attack range.

### Moment and Centers-of-Pressure Results

The chordwise center of pressure and pitching moment for both wings are shown in figure 7. The chordwise center of pressure for both wings moves rearward with increasing angle of attack as predicted by all methods except linear theory which does not predict any shift with angle of attack. It is shown in the pitching-moment plots that 4- or 5-percent root-chord disagreement in the center-of-pressure predictions makes a large discrepancy in the pitching-moment predictions as the experimental center of pressure is so near the pitching-moment reference ( $0.5\bar{c}$ ). Even though the linear theory predicts no center-of-pressure shift with change in angle of attack, the linear-theory predictions give the closest approximation to experimental results which show a movement of only  $\pm 4$  percent of the wing-root chord.

The spanwise center of pressure and the wing-root bending moment are shown in figure 8 for both wings. The experimental center of pressure shows a general inboard movement with increasing angle of attack; as all of the theoretical methods make no allowance for spanwise center of pressure shift with change in angle of attack, they are all equally limited in their usefulness. For this investigation the predictions are within  $\pm 7$  percent wing semispan of the experimental centers of pressure.

A plot of the two-dimensional center-of-pressure travel for both wings is shown as figure 9. Here the inboard, rearward movement of the center of pressure with increasing angle of attack is clearly shown. For wing 1 at the higher angles, the center of pressure begins to return outboard. This indication is the same as that shown for very low-aspect-ratio wings at lower Mach numbers. (See refs. 7 and 8.)

## Lift-Drag-Ratio Results

Plots of lift-drag ratio are shown for both wings as figure 11. Maximum  $L/D$  occurs at approximately  $\alpha = 6^\circ$  for wing 1 and at  $\alpha = 4^\circ$  for wing 2. Despite the limitations being exceeded for the lift and drag predictions, all the theoretical methods except the Newtonian-impact theory give very good predictions of the lift-drag ratio.

## CONCLUSIONS

Wind-tunnel tests of two low-aspect-ratio double-wedge delta wings in the Langley 9- by 9-inch Mach number 4 blowdown jet at a Mach number of 4.07 and comparisons of the experimental data with lower Mach number tests and with several theoretical methods indicate the following conclusions:

1. The maximum lift coefficient  $C_{L_{\max}}$  for low-aspect-ratio delta wings decreases with increasing Mach number.

2. The angle of attack for the maximum lift coefficient  $\alpha_{C_{L_{\max}}}$  for low-aspect-ratio delta wings increases with increasing Mach number to at least a Mach number of 4.07.

3. Although probably fortuitously, linear theory gives generally the best predictions for all the aerodynamic data obtained in the present tests.

4. The center of pressure for delta wings moves inboard and rearward with increasing angle of attack, and for very low-aspect-ratio ( $A < 2$ ) delta wings at high angles of attack ( $\alpha > 35^\circ$ ) begins to return outboard while still moving rearward.

Langley Aeronautical Laboratory,  
National Advisory Committee for Aeronautics,  
Langley Field, Va., April 12, 1957.

## REFERENCES

1. Love, Eugene S.: Investigations at Supersonic Speeds of 22 Triangular Wings Representing Two Airfoil Sections for Each of 11 Apex Angles. NACA Rep. 1238, 1955. (Supersedes NACA RM L9D07.)
2. Vincenti, Walter G., Nielsen, Jack N., and Matteson, Frederick H.: Investigation of Wing Characteristics at a Mach Number of 1.53. I - Triangular Wings of Aspect Ratio 2. NACA RM A7I10, 1947.
3. Ellis, Macon C., Jr., and Hasel, Lowell E.: Preliminary Investigation at Supersonic Speeds of Triangular and Sweptback Wings. NACA TN 1955, 1949.
4. Ulmann, Edward F., and Dunning, Robert W.: Aerodynamic Characteristics of Two Delta Wings at Mach Number 4.04 and Correlations of Lift and Minimum-Drag Data for Delta Wings at Mach Numbers From 1.62 to 6.9. NACA RM L52K19, 1952.
5. Dunning, Robert W., and Smith, Fred M.: Aerodynamic Characteristics of Two Delta Wings and Two Trapezoidal Wings at Mach Number 4.04. NACA RM L53D30a, 1953.
6. Gallagher, James J., and Mueller, James N.: An Investigation of the Maximum Lift of Wings at Supersonic Speeds. NACA Rep. 1227, 1955. (Supersedes NACA RM L7J10.)
7. Kaattari, George E.: Pressure Distributions on Triangular and Rectangular Wings to High Angles of Attack - Mach Numbers 1.45 and 1.97. NACA RM A54D19, 1954.
8. Kaattari, George E.: Pressure Distributions on Triangular and Rectangular Wings to High Angles of Attack - Mach Numbers 2.46 and 3.36. NACA RM A54J12, 1955.
9. Dorrance, William H.: Two-Dimensional Airfoils at Moderate Hypersonic Velocities. Jour. Aero. Sci., vol. 19, no. 9, Sept. 1952, pp. 593-600.
10. Ulmann, Edward F., and Lord, Douglas R.: An Investigation of Flow Characteristics at Mach Number 4.04 Over 6- and 9-Percent-Thick Symmetrical Circular-Arc Airfoils Having 30-Percent-Chord Trailing-Edge Flaps. NACA RM L51D30, 1951.
11. Ivey, H. Reese, Stickle, George W., and Schuettler, Alberta: Charts for Determining the Characteristics of Sharp-Nose Airfoils in Two-Dimensional Flow at Supersonic Speeds. NACA TN 1143, 1947.

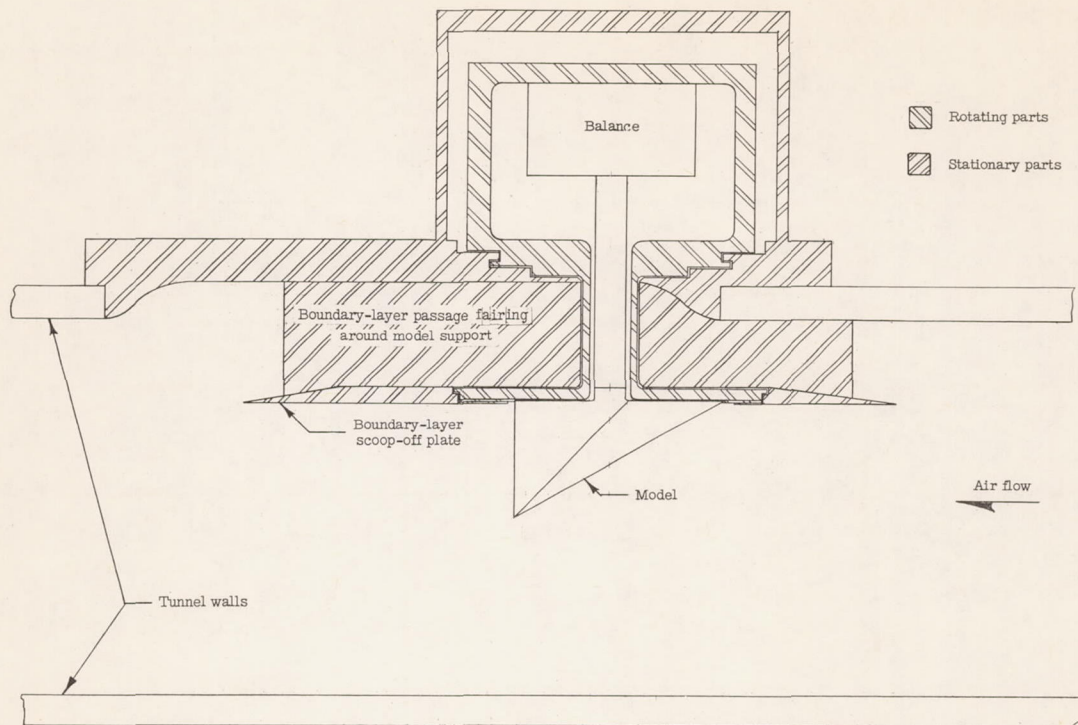
12. Bertram, Mitchel H., and McCauley, William D.: Investigation of the Aerodynamic Characteristics at High Supersonic Mach Numbers of a Family of Delta Wings Having Double-Wedge Sections With the Maximum Thickness at 0.18 Chord. NACA RM L54G28, 1954.
13. Van Driest, E. R.: Investigation of Laminar Boundary Layer in Compressible Fluids Using the Crocco Method. NACA TN 2597, 1952.
14. Van Driest, E. R.: The Turbulent Boundary Layer for Compressible Fluids on a Flat Plate With Heat Transfer. Rep. No. AL-997, North American Aviation, Inc., Jan. 27, 1950.
15. Boatright, William B.: Experimental Study and Analysis of Loading and Pressure Distributions on Delta Wings Due to Thickness and to Angle of Attack at Supersonic Speeds. NACA RM L56I14, 1956.
16. Ulmann, Edward F., and Bertram, Mitchel H.: Aerodynamic Characteristics of Low-Aspect-Ratio Wings at High Supersonic Mach Numbers. NACA RM L53I23, 1953.
17. Ulmann, Edward F., and Smith, Fred M.: Aerodynamic Characteristics of a  $60^\circ$  Delta Wing Having a Half-Delta Tip Control at a Mach Number of 4.04. NACA RM L55A19, 1955.
18. Nielson, Jack N., Spahr, J. Richard, and Centolanzi, Frank: Aerodynamics of Bodies, Wings, and Wing-Body Combinations at High Angles of Attack and Supersonic Speeds. NACA RM A55L13c, 1956.

TABLE I

## EXPERIMENTAL AND THEORETICAL WING PARAMETERS

Wing 1; aspect-ratio-1.33 delta wing; $\epsilon = 18.4^\circ$			
	$C_{L\alpha}$	$C_{D0}$ (1)	$(L/D)_{\max}$
Experiment	0.0150	0.0093	4.78
Linear theory	.0177	.0117	4.65
Shock-expansion theory	.0185	.0108	4.95
Newtonian-impact theory	.0050	.0052	3.35
Dorrance's method (ref. 9)	.0189	.0107	4.57
Wing 2; aspect-ratio-2.31 delta wing; $\epsilon = 30^\circ$			
Experiment	0.0184	0.0061	6.57
Linear theory	.0177	.0065	6.16
Shock-expansion theory	.0177	.0064	6.31
Newtonian-impact theory	.0029	.0040	3.81
Dorrance's method (ref. 9)	.0180	.0060	6.25

<sup>1</sup>All theoretical predictions for  $C_{D0}$  contain a skin-friction drag coefficient computed from references 13 and 14 (0.0043 for wing 1 and 0.0038 for wing 2).



Section A-A

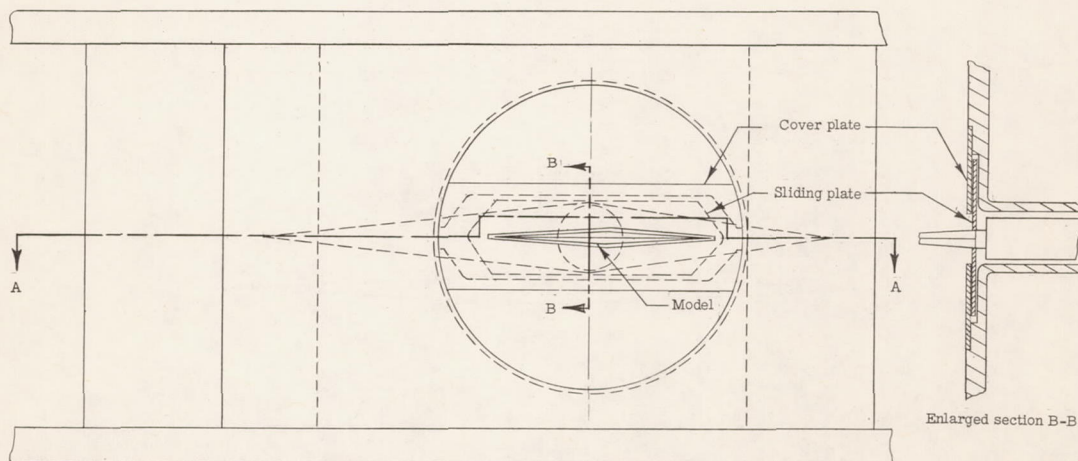


Figure 1.- Schematic diagram of Langley 9- by 9-inch Mach number 4 blow-down jet showing model and balance arrangement.

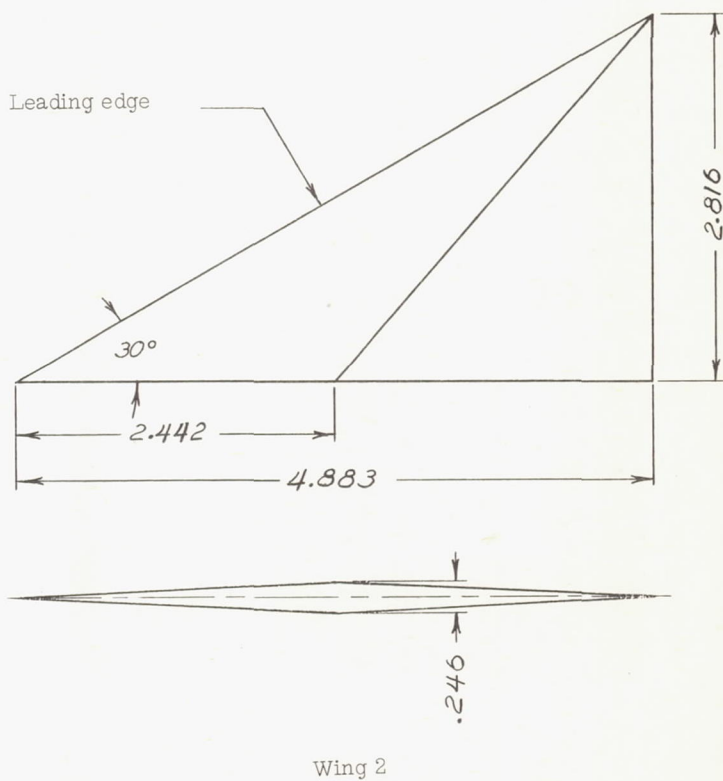
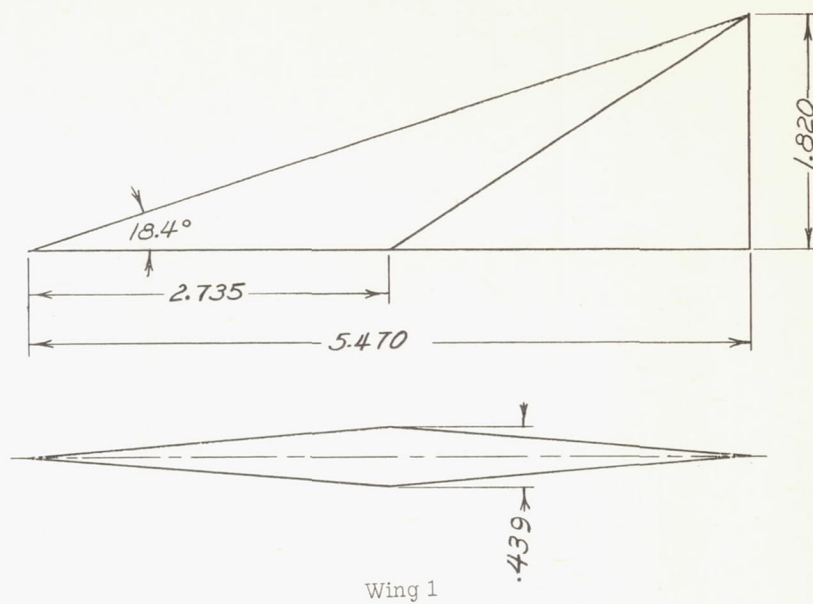
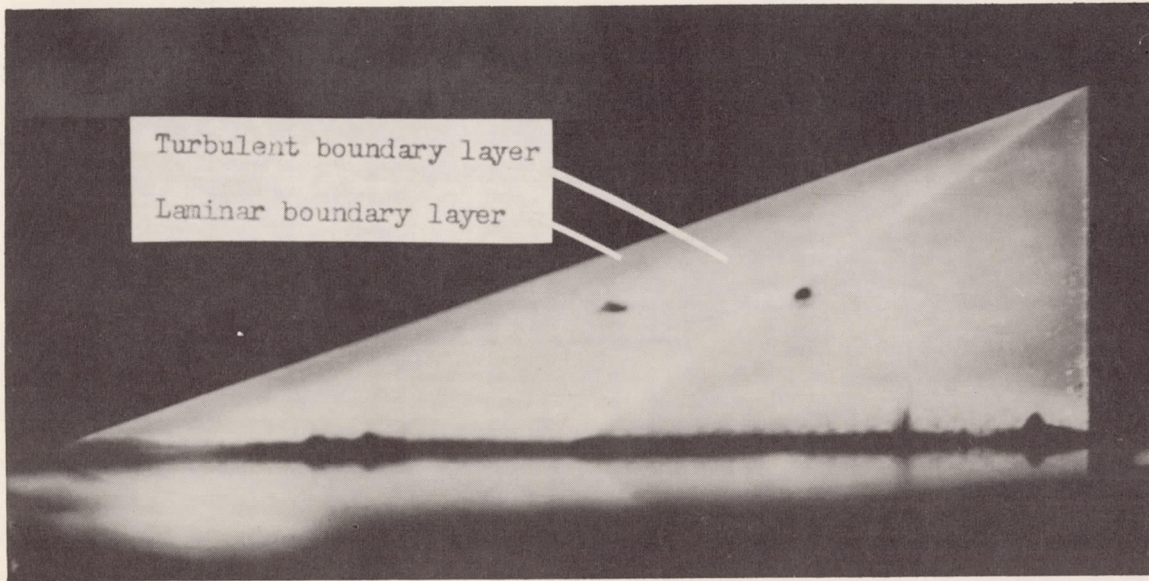


Figure 2.- Schematic diagrams of test wings. Dimensions are in inches.



L-57-1568  
Figure 3.- Photograph of wing 1 showing the regions of laminar and turbulent boundary layer.

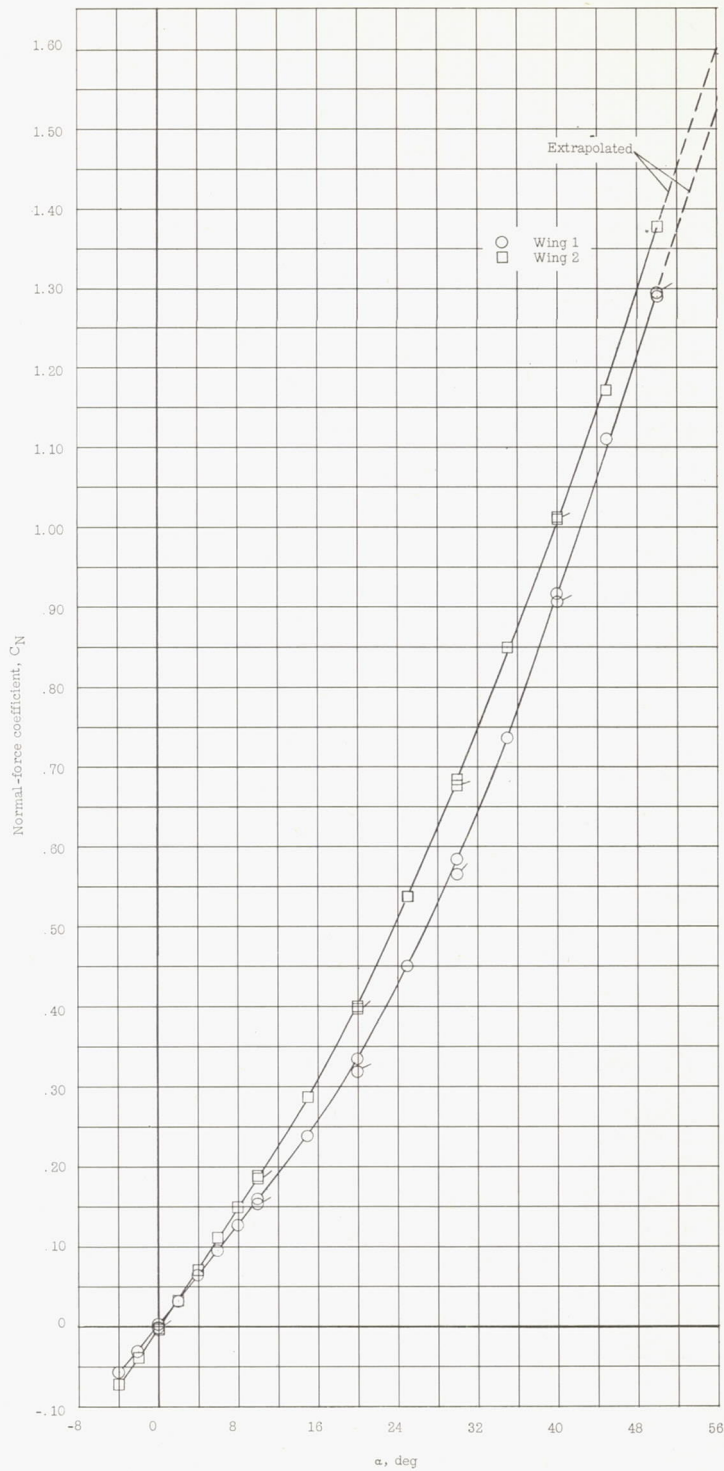
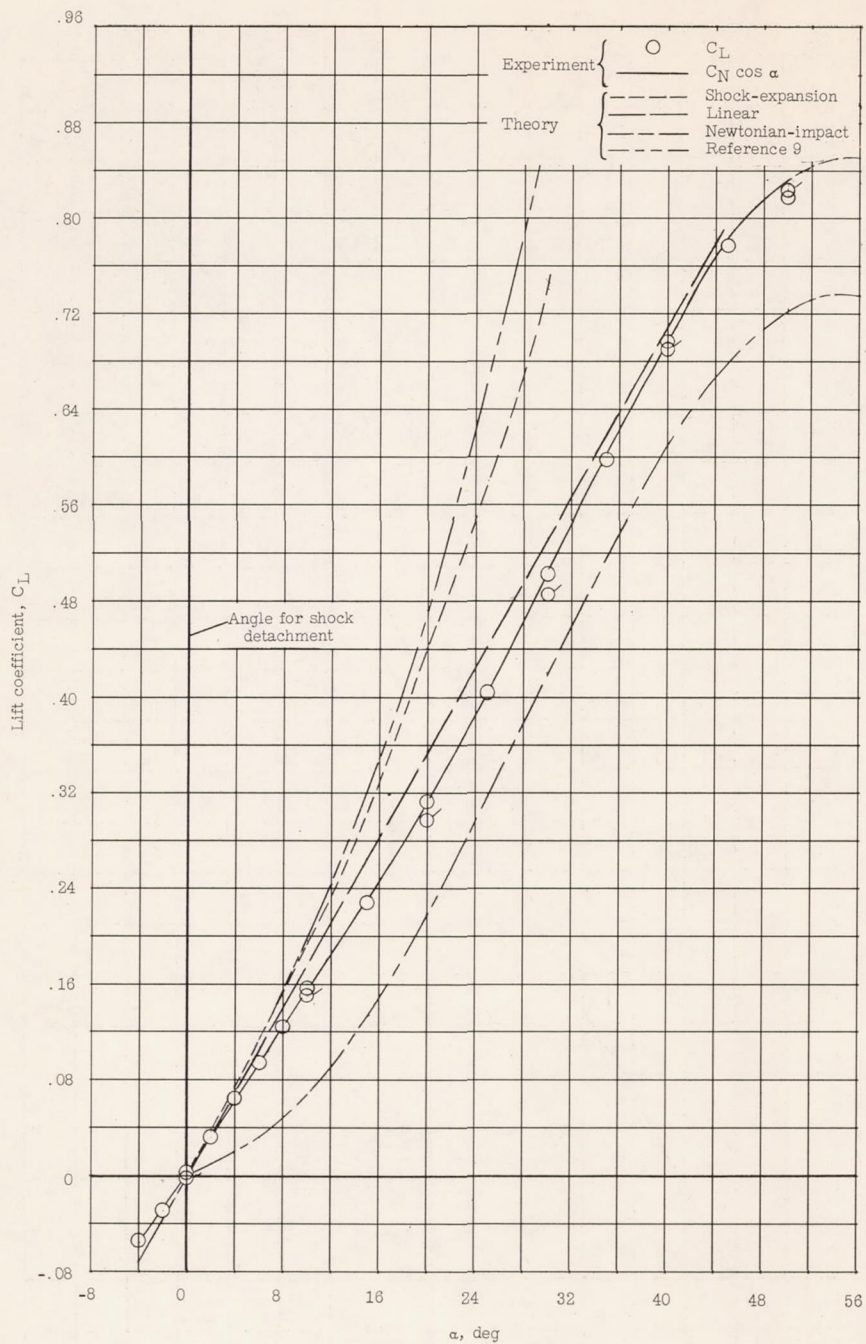
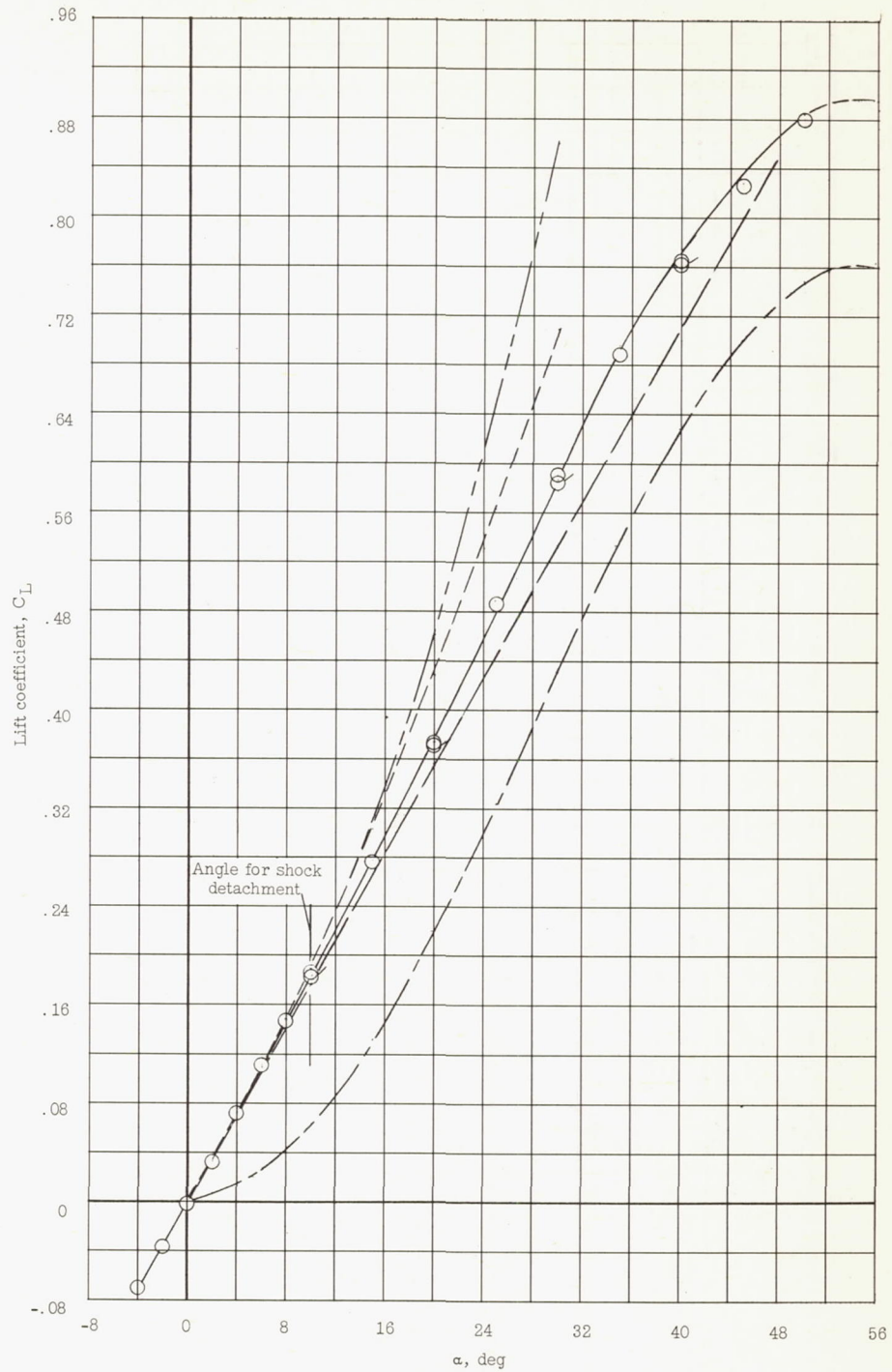


Figure 4.- Normal-force coefficients of two delta wings at  $M = 4.07$ .  
Flagged symbols represent check points.



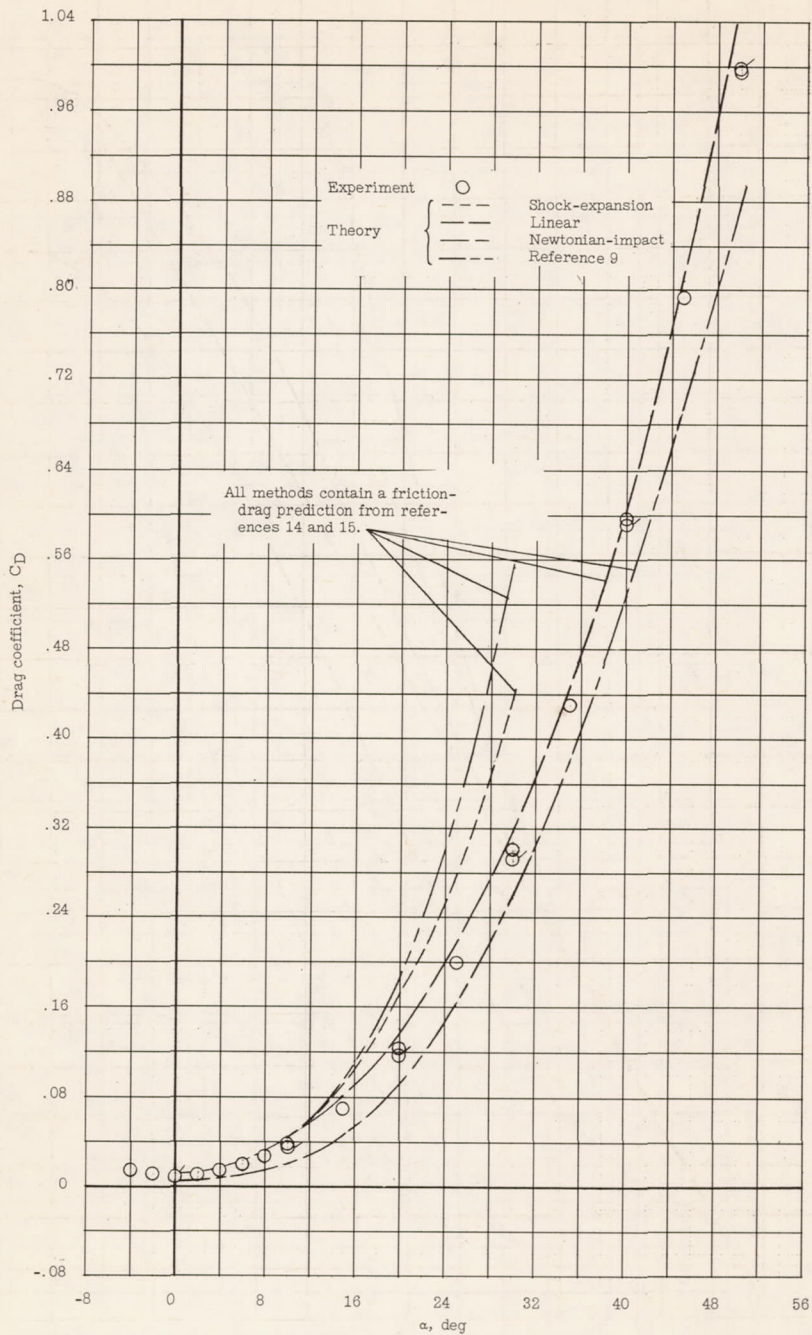
(a) Wing 1.

Figure 5.- Lift coefficients of two delta wings at  $M = 4.07$ . Flagged symbols represent check points.



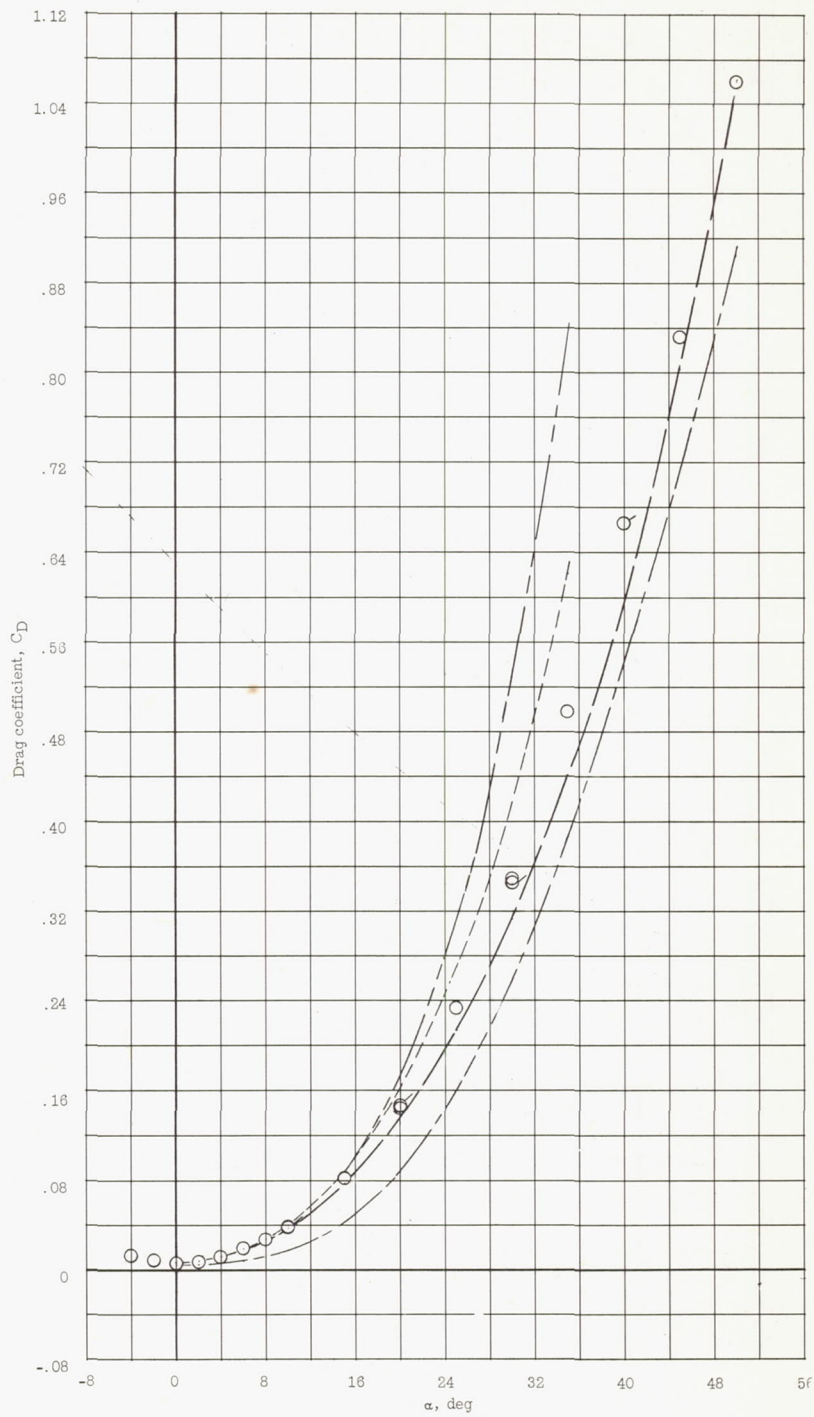
(b) Wing 2.

Figure 5.- Concluded.



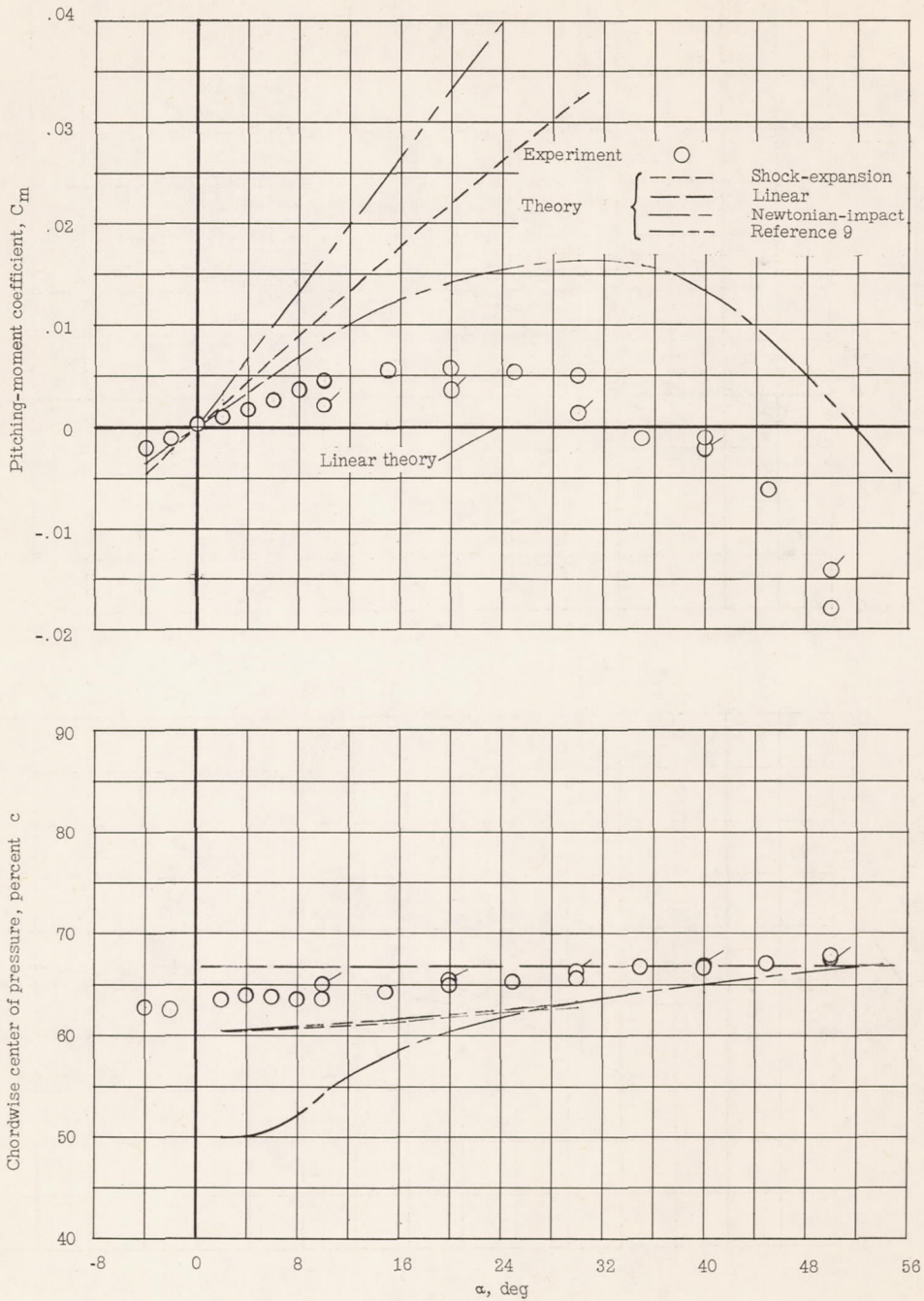
(a) Wing 1.

Figure 6.- Drag coefficients of two delta wings at  $M = 4.07$ . Flagged symbols represent check points.



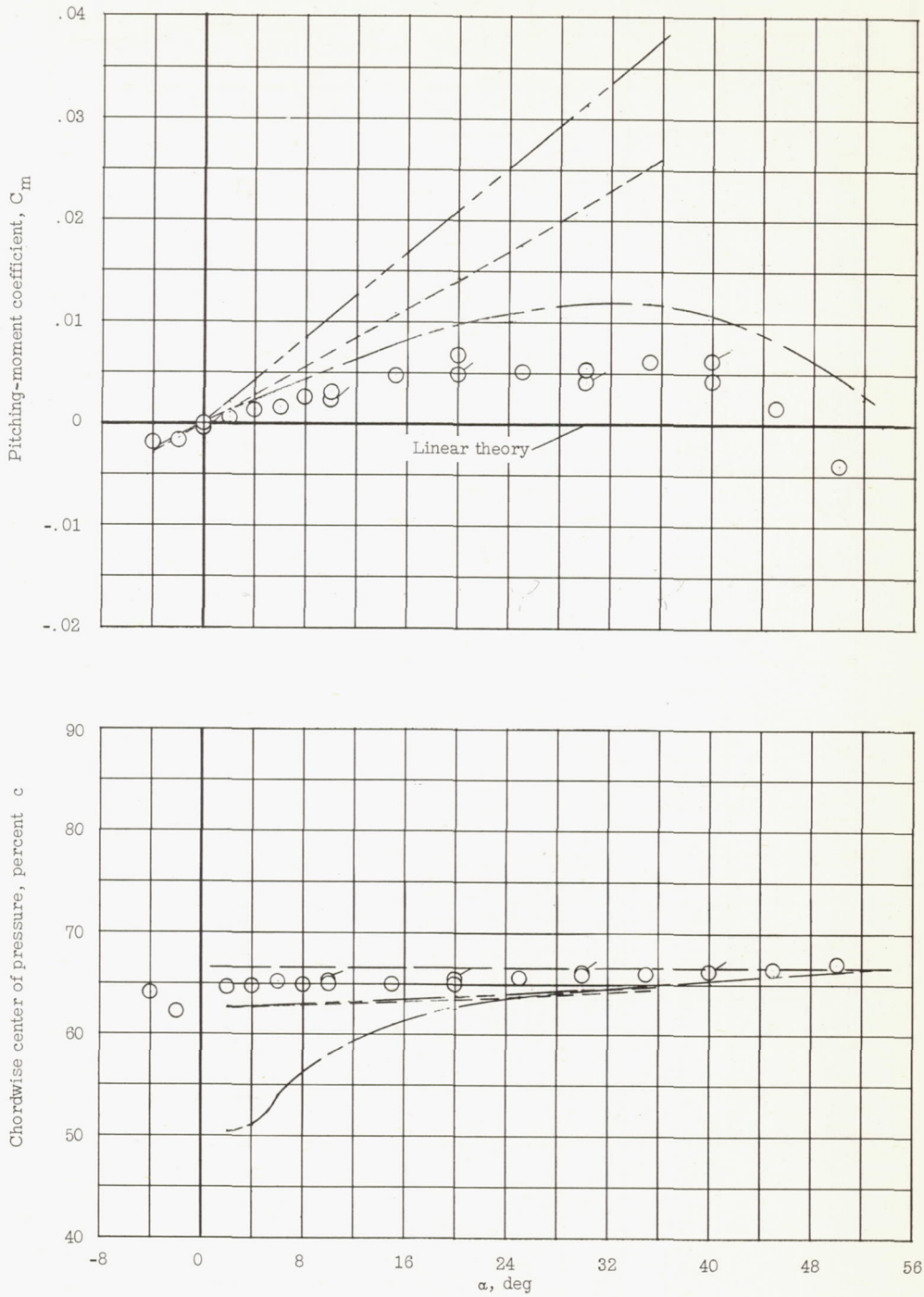
(b) Wing 2.

Figure 6.- Concluded.



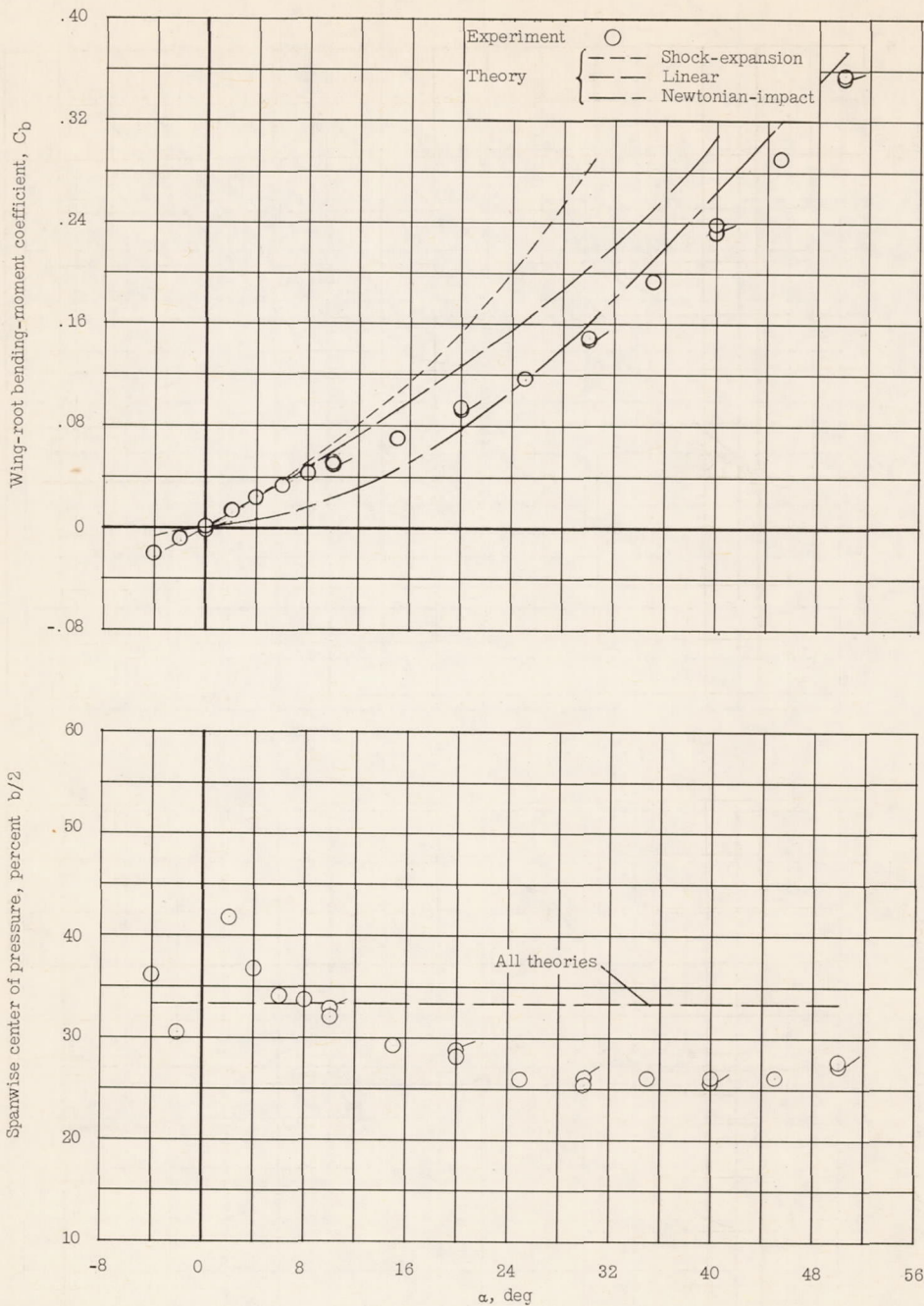
(a) Wing 1.

Figure 7.- Pitching moment and chordwise center of pressure of two delta wings at  $M = 4.07$ . Flagged symbols represent check points.



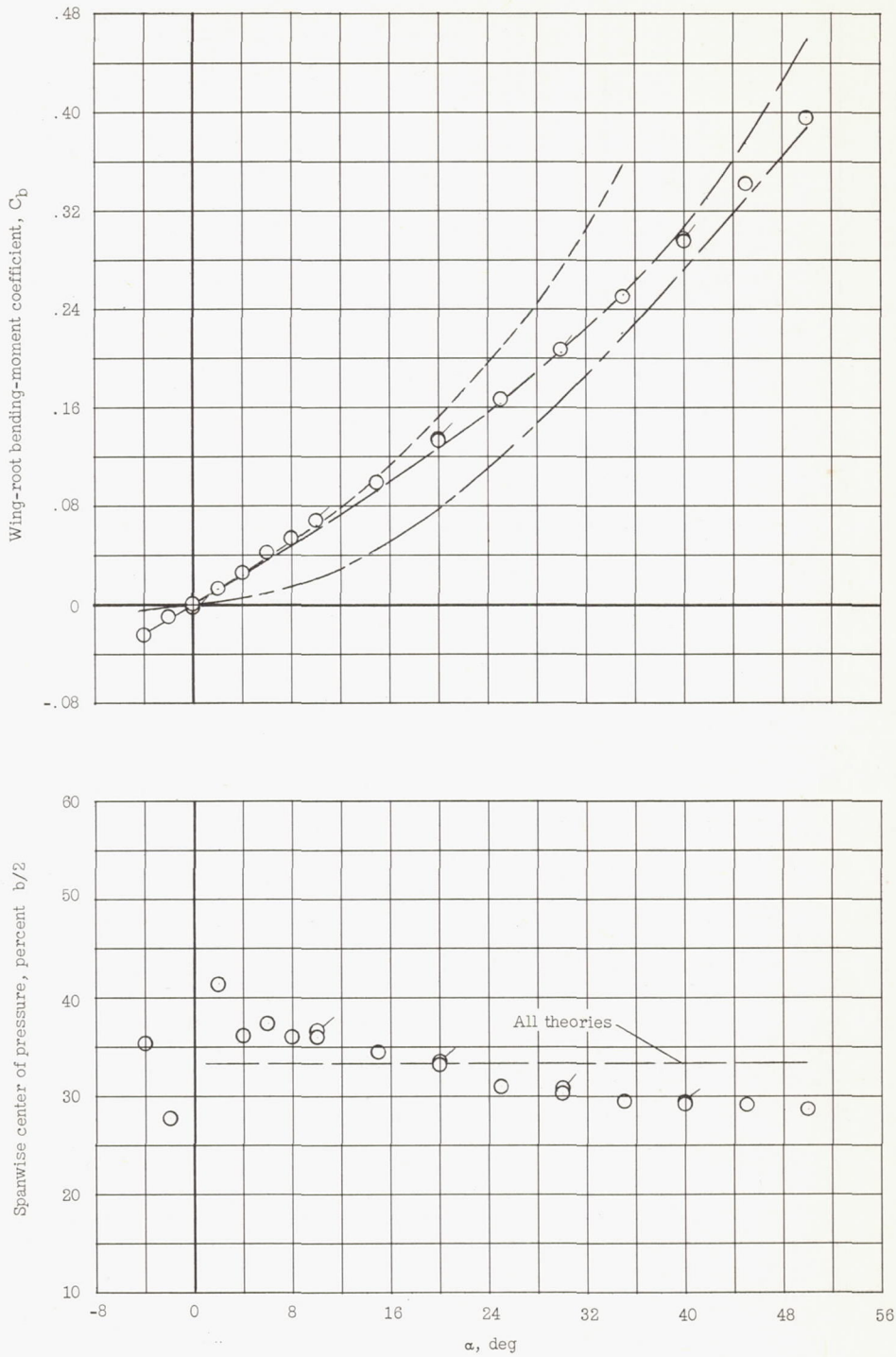
(b) Wing 2.

Figure 7.- Concluded.



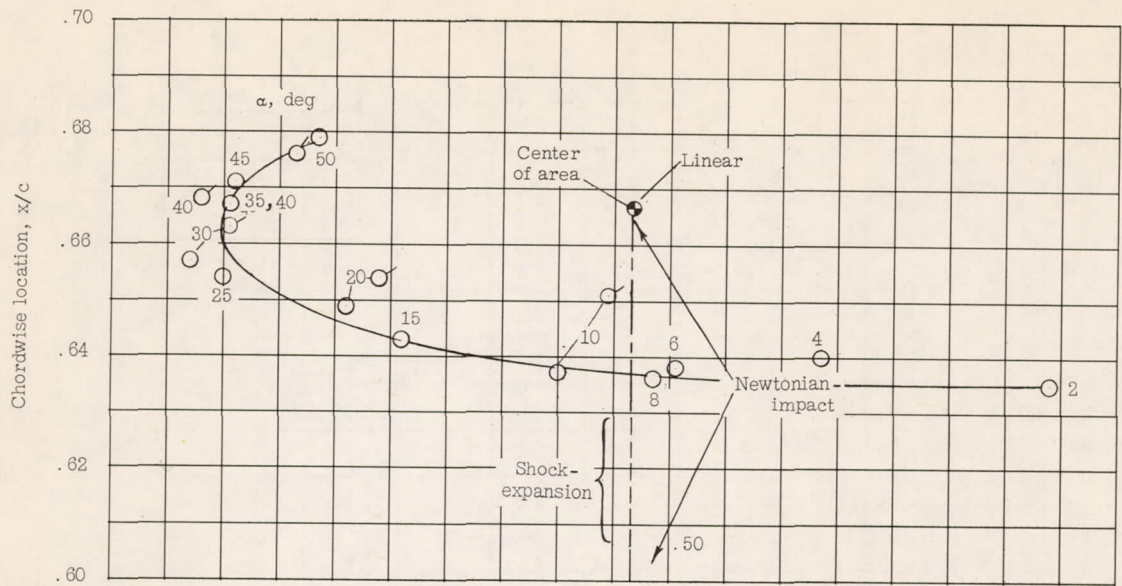
(a) Wing 1.

Figure 8.- Wing-root bending moments and spanwise centers of pressure of two delta wings at  $M = 4.07$ . Flagged symbols indicate check points.

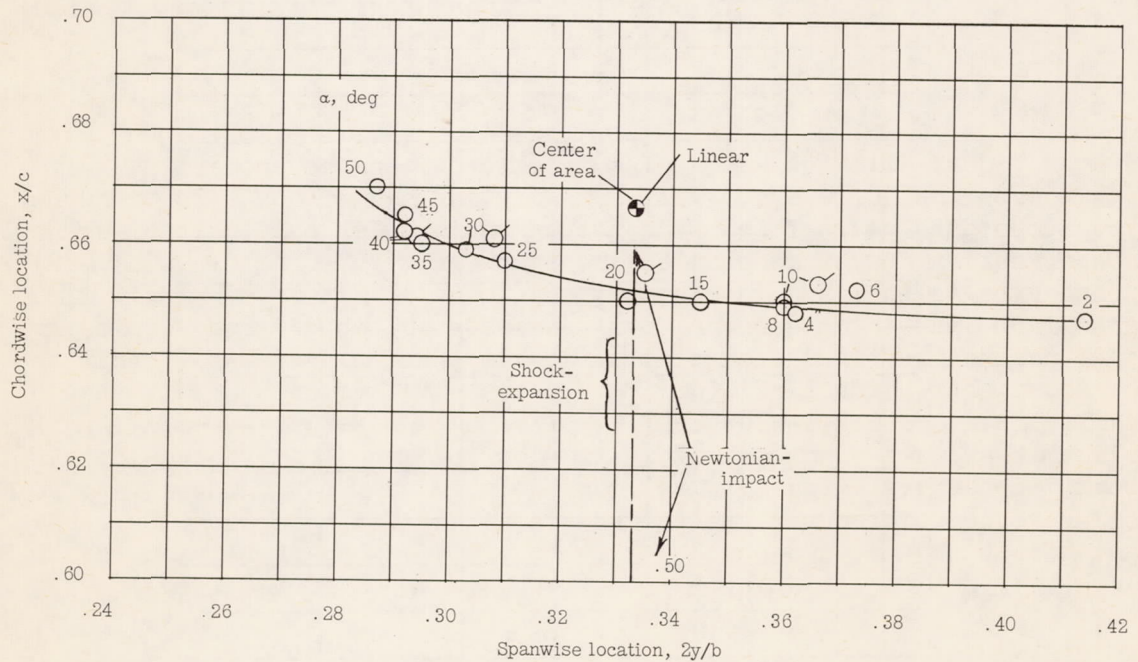


(b) Wing 2.

Figure 8.- Concluded.

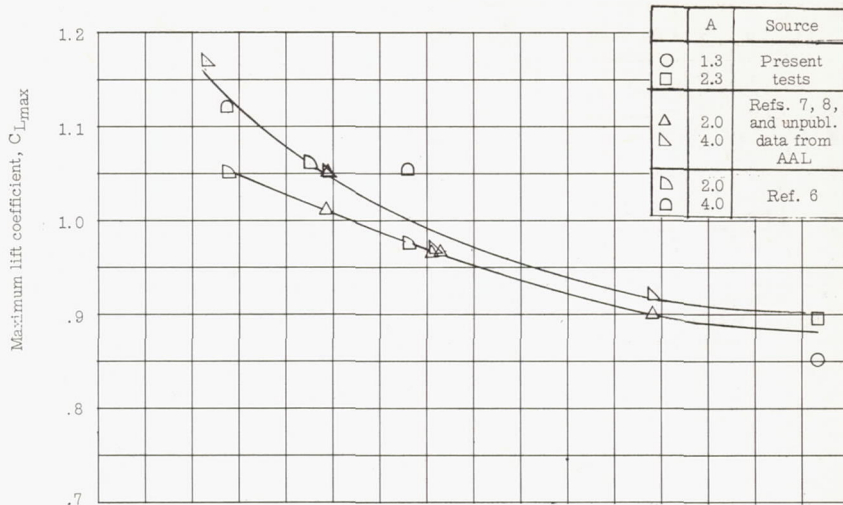


(a) Wing 1.

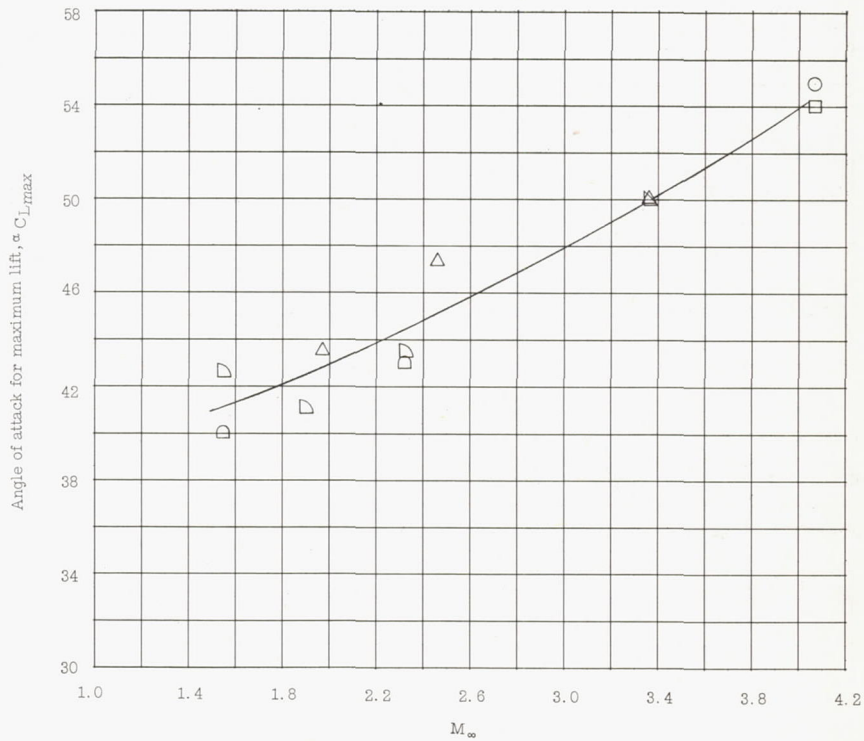


(b) Wing 2.

Figure 9.- Center-of-pressure travel for two delta wings at  $M = 4.07$ . Flagged symbols indicate check points.

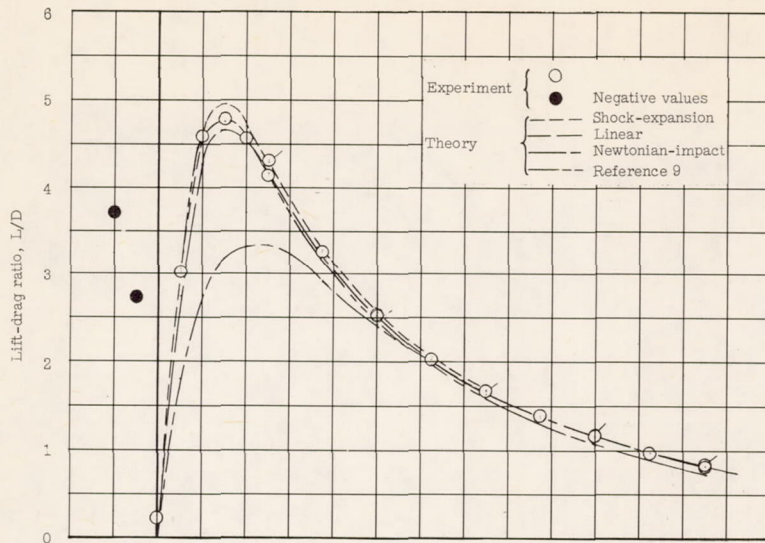


(a) Maximum lift coefficient.

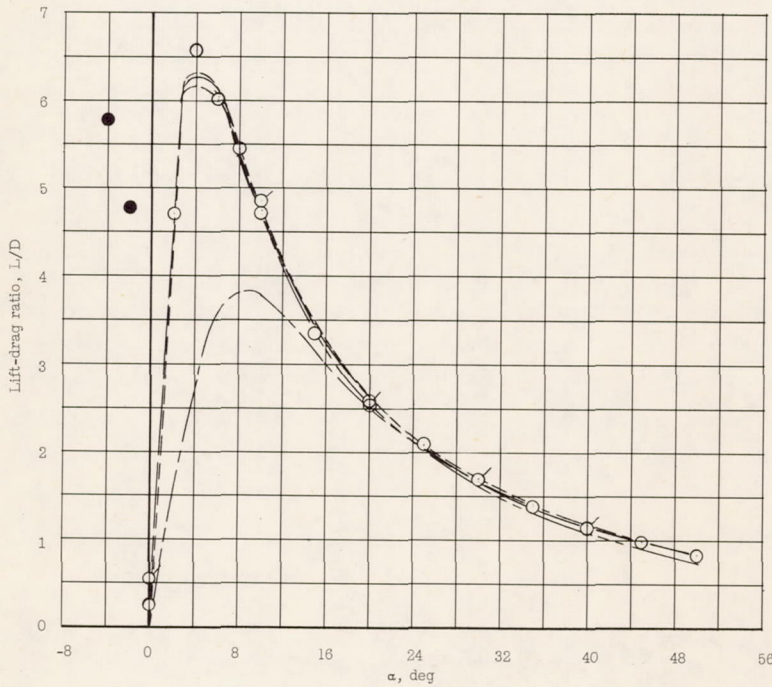


(b) Angle of attack for maximum lift.

Figure 10.- Effect of Mach number on maximum lift of several low-aspect-ratio delta wings.



(a) Wing 1.



(b) Wing 2.

Figure 11.- Lift-drag ratios of two delta wings at  $M = 4.07$ . Flagged symbols indicate check points.